Journal of the European Ceramic Society **17** (1997) 1565–1572

PII: S0955-2219(97)00014-9
0955-2219/97/$17.00

The Role of Residual Stress on the Mechanical Properties of Al_2O_3–5 vol% SiC Nano-Composites

J. Luo & R. Stevens

School of Materials Science, University of Bath, Bath, UK, BA2 7AY

(Received 1 April 1996; revised version received 19 December 1996; accepted 3 January 1997)

Abstract

The role of nano-sized SiC particles in Al_2O_3–5 vol% SiC nano-composites is still a topical subject. As yet there is little agreement on the mechanisms of mechanical property enhancement in such composites. However, the significance of the residual stresses generated by the thermal expansion mismatch between the matrix and SiC in the composites is generally appreciated. The large shear stress generated plays a dominant role in the generation and movement of dislocations, especially during thermal treatment. It is possible that dislocation movement could also result in the microcrack healing, which contributes to the strength enhancement. The high value of the tensile residual hoop stress in the matrix is the major contribution to the transgranular fracture in the composites. The high compressive radial residual stress in the matrix contributes both to crack pinning and also crack bridging to enhance the strength and toughness. Both the radial and hoop residual stresses can help crack deflection. © 1997 Elsevier Science Limited.

1 Introduction

Addition of sub-micron particles to form a second phase is expected to improve the mechanical properties of ceramics. A significant increase in the mechanical properties was reported by Niihara *et al.*[1–3] in the 5 vol% nano-sized SiC particles reinforced alumina. The strength was raised from 350 MPa for monolithic Al_2O_3 to over 1 GPa. The strength was further increased to 1·5 GPa after thermal treatment. The toughness also improved, from 3·3 MPa $m^{1/2}$ to 4·7 MPa $m^{1/2}$. Other research groups also found that addition of SiC increased the strength and that a thermal treatment further improved strength.[4–6] However, their observations indicated that the strength increment was much less dramatic,[4–6] for instance, a 30–40% increase in strength was observed by the group from Lehigh University but not the 300% reported earlier.[1–3]

Disagreement still remains concerning the role of nano-size inclusions in the enhancement of mechanical properties of the nano-composites, although it is generally accepted that the pinning effect of the nano-size particles is the key factor influencing the improvement of high-temperature properties and wear resistance.[7,8] Pezzotti *et al.*[9] discussed the nano-composites using traditional fracture mechanics and pointed out that the inherent toughness and strength would not be expected to be high. Niihara *et al.*[1–3] attributed the significant improvement of the strength of Al_2O_3–5 vol% SiC composites to the presence of sub-grain boundaries formed by dislocation bands in the thermally annealed materials and to the small dimensions of the inherent flaws. The dislocation bands have also been observed in the same material by Jiao *et al.*[10] and Levin.[11]

On the other hand, the group from Lehigh University[4,12,13] gave a quite different interpretation of the strength enhancement. Their explanation is based on the occurrence of micro-cracking and residual stress, generated by diamond machining processes. In monolithic alumina, the residual stress can be relieved by thermal annealing, but any machining cracks present remain and even grow during the stress relief. However, in the case of nano-composites, the thermal anneal may help crack healing and yet only partially relieve the residual stress. Recently, Chou *et al.*[14] reported that the surface residual stress induced by machining in the nano-composites is of a similar nature to that generated in monolithic Al_2O_3, and concluded that the residual machining stress could not be the major contribution to the strength increment in the composites. Borsa *et al.*[5] attributed the strength enhancement simply to the grain refinement and change in fracture mode.

Nevertheless, it is accepted that the residual stresses[11,15,16] generated by mismatch of thermal expansion coefficients between the matrix and

inclusions play an important role in determining the mechanical properties of the ceramic nano-composites, including the change in fracture mode and the generation and movement of dislocations. There has been, however, little or no systematic discussion of the role played by the residual stress in the composites. Generally speaking, the residual stress occurs in virtually any composite, at micro or nano component scale, and the level generated is determined by the nature, size and volume fraction of the inclusions. In the present study, the authors specifically discuss the role of the residual stresses in ceramic nano-composites, and include a calculation of the residual stress in the composites, with particular reference to the important and debatable operative mechanisms of the 5 vol% SiC reinforced Al_2O_3 composites.

2 Average residual stress

The residual stresses in a composite are often generated by the mismatch of the thermal expansion coefficient (TEC) between the matrix and inclusions. Any difference in elastic moduli can also affect the residual stress. The average stress in the composites can be evaluated using the Eshelby model[17] in combination with the Mori–Tanaka law[18] in the inclusion composites (see Refs 19, 20). In the case of low volume fractions of inclusion content, the residual stress for spherical inclusion composites (which can approximate to the nano-composites) can be evaluated by following expressions:[20]

$$\langle\sigma\rangle_M = \frac{12FK_MG_MK_I}{K_M(3K_I + 4G_M) + 4FG_M(K_I - K_M)}\varepsilon^T \quad (1a)$$

$$\langle\sigma\rangle_I = -\frac{12(1-F)K_MG_MK_I}{K_M(3K_I + 4G_M) + 4FG_M(K_I - K_M)}\varepsilon^T \quad (1b)$$

where the subscripts, M and I are for the matrix and the inclusions, K and G are the bulk and shear moduli of materials, F is the volume fraction of the inclusions, ε^T is the constraint strain, generated usually by mismatch of the TEC between matrix and inclusions.

Selection of the appropriate elastic moduli for Al_2O_3 and SiC can affect the value of the residual stress. There are a number of reports available detailing the elastic moduli of both components. The crystallographic similarity of the polytypes of SiC results in the overall elastic moduli of the polytypes having similar values.[21,22] The Voigt and Reuss bounds were calculated from the elastic constants of SiC, and the average values of the two bounds are used to represent the aggregate moduli for SiC, as listed in Table 1.

Since the SiC nano-particles are located within the Al_2O_3 matrix, the elastic constants of single crystalline Al_2O_3 need to be considered in relation to the calculation of the residual stress. Several authors have compared elastic constants of both single and polycrystalline Al_2O_3[23–25] and obtained the aggregated bulk and shear moduli of the material, related to temperature, as listed in Table 1. The contribution of elastic mismatch between SiC and Al_2O_3 on the residual stress in the composites can be calculated to be –5·5% of the total with the temperature dependence having little effect.

The residual stresses in the composites are proportional to the constraint strain. Ceramic-ceramic composites are generally fabricated at high temperature. At the sintering temperature, the structural rearrangement which takes place and the sintering process do not generate significant residual stresses. However, on cooling, as the temperature is reduced, the creep rate decreases exponentially with temperature and the structural rearrangement will, due to reduced rate processes, be unable to adjust to the difference in the shrinkage between the inclusions and matrix at a specific temperature, which can be termed the threshold temperature, T_0. T_0 is always below the sintering temperature and can be dependent on the cooling rate. The constraint strain at temperature T, is given by:

$$\varepsilon^T = \int_{T_0}^{T} (\alpha_I - \alpha_M)dT \quad (2)$$

where α_I and α_M are the TECs of inclusion and matrix, respectively. In the case of Al_2O_3/SiC nano-composites, two polytypes of SiC particles (α, hexagonal, β, cubic) have been used as the

Table 1. Some relevant parameters of SiC and Al_2O_3

	SiC	*Al_2O_3*
TEC (10^{-6}/°C)	α-SiC $\alpha_I = 3{\cdot}24 + 3{\cdot}25 \times 10^{-3}T - 1{\cdot}36 \times 10^{-6}T^2$ α-SiC $\alpha_I = 3{\cdot}12 + 3{\cdot}6 \times 10^{-3}T - 1{\cdot}68 \times 10^{-6}T^2$	Polycrystalline $\alpha_M = 6{\cdot}48 + 5{\cdot}06 \times 10^{-3}T - 2{\cdot}35 \times 10^{-6}T^2$ Sapphire $\alpha_c = 6{\cdot}85 + 5{\cdot}78 \times 10^{-3}T - 2{\cdot}75 \times 10^{-6}T^2$ $\alpha_a = 6{\cdot}04 + 5{\cdot}60 \times 10^{-3}T - 2{\cdot}68 \times 10^{-6}T^2$
Elastic modulus (GPa)	$K_I = 225 - 0{\cdot}0015T$ $G_I = 200 - 0{\cdot}029T$	$K_M = 253 - 0{\cdot}0173T$ $G_M = 164 - 0{\cdot}0223T$

reinforcing phase. The similarity in the local tetrahedral bonding in both the cubic and hexagonal SiC polytypes results in the overall thermal expansion coefficients of the polytypes being similar,[26–29] as shown in Table 1. Thus the average value for the α and β polytypes can be used to represent the TEC of SiC. The TEC of Al_2O_3[30–33] is also given in Table 1.

In order to obtain a value for the constraint strain using eqn (2) it is important to select the correct threshold temperature T_0. Todd *et al.*[15] measured the average residual stress in Al_2O_3/SiC nano-composites using neutron diffraction, and indicated that the critical temperature is higher than 1300°C. Fang *et al.*[12] and Thompson *et al.*[13] heat treated the nano-composites at 1300°C and found that the indentation residual stress was only partially relieved at this temperature. This evidence also supports the suggestion that the threshold temperature for stress relaxation is higher than 1300°C. Evans and co-workers[34] have discussed the residual stress generated by anisotropy in the Al_2O_3 grains in terms of the Eshelby model, in which the threshold temperature was assumed to be 1500°C, which was also used for the threshold temperature in this composite. In this case, the constraint strain in the composites is:

$$\varepsilon^R = 5{\cdot}85 \times 10^{-3} - 3{\cdot}3 \times 10^{-6}T - 0{\cdot}82 \times 10^{-9}T^2 \quad (3)$$

In order to verify the estimate for the threshold temperature, we can compare an evaluation of the residual stress in nano-size SiC particle composites with the experimental results reported by Levin *et al.*,[11] as shown in Fig. 1. The TEC of an α-SiC particle is used in the calculation, since the experiments were based on α-SiC composites. The evaluations are in reasonable agreement with the experimental results.

3 Residual stress in the matrix

The average residual stress in the inclusions can approximate the residual stresses in the inclusion composites. The average residual stress in the matrix may be used to explain the residual stress distribution for high inclusion contents, apart from the interfacial areas, where a large deviation can be generated between the average value and the localised stress. When the volume fraction of the inclusions is very low, the average residual stress in the matrix will differ considerably from the localised residual stress distribution.

At low inclusion volume fractions, for example 5 vol%, the inter-particle spacing is approximately 2·7 times their size, when it may be assumed that the residual stresses at a point in the matrix are generated only by the nearest inclusion. The composite spherical model (CSM),[35,36] can thus be used to evaluate the residual stresses in the matrix (see Appendix). The core is represented by the inclusion, while the shell is the matrix. The thickness of the shell, t, is given by: $t = r\,F^{-1/3}(1 - F^{1/3})$, (where r is the inclusion radius). For 5 vol% of inclusions, the thickness of the shell is $1{\cdot}71r$. The residual stress in the core can be calculated by the CSM model and is the same as obtained using the Eshelby model, eqn (1b); the stresses in the shell are given by:

$$\sigma_R = \frac{(r/R)^3 - F}{1 - F}\,\sigma_I \qquad (r < R < r + t) \quad (4a)$$

$$\sigma_T = \frac{0{\cdot}5(r/R)^3 + F}{1 - F}\,\sigma_I \qquad (r < R < r + t) \quad (4b)$$

Figure 2 shows the residual stress in the matrix between two particles, calculated using eqn (4).

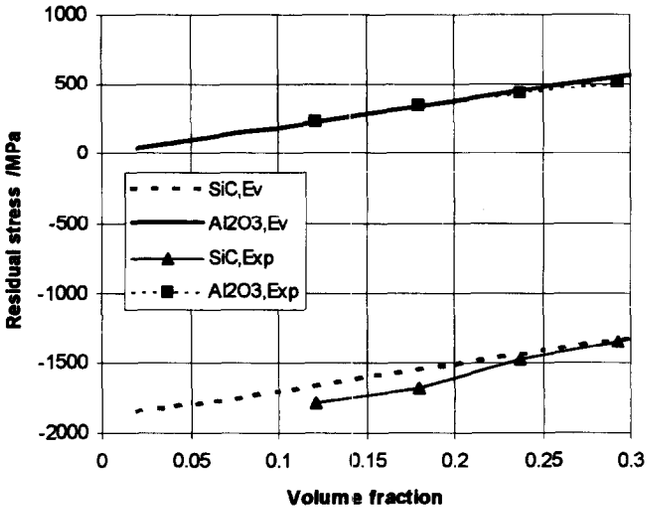

Fig. 1. Comparison of the average residual stresses in Al_2O_3 and SiC between the values calculated (*Al_2O_3, Ev* and *SiC, Ev*) using eqn (1) and the experimental results (*Al_2O_3, Exp* and *SiC, Exp*) of Levin *et al.* (Ref. 11).

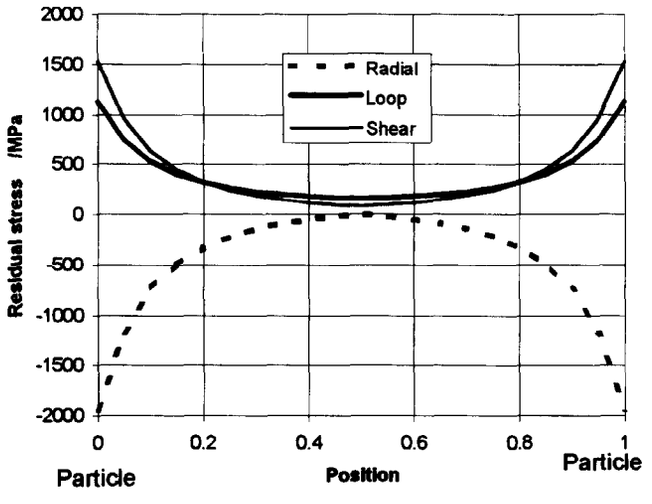

Fig. 2. Residual stress distribution in the matrix of Al_2O_3–5 vol% SiC nano-composites between two particles. Positions 0 and 1 are two interfaces between the matrix and the particles.

It is apparent that the residual stress near the inclusions is high, and at a distance from the inclusions the stress decreases dramatically. It would be expected that the high tensile loop stress plays an important role in the change of fracture mode, from intergranular fracture in monolithic Al_2O_3 to the transgranular fracture in the nano-composites.

3.1 Refinement of the residual stress

Corundum has two quite different thermal expansion coefficients in the directions parallel and vertical to the c-axis: α_c, α_a, (see Table 1). The TEC of corundum in any direction can be evaluated using α_c and α_a in the following equation:

$$\alpha_\theta = \alpha_c \cos^2\theta + \alpha_a \sin^2\theta \qquad (5)$$

where θ is the angle between the direction and c-axis.

Most of the SiC particles are located within the Al_2O_3 grains in the Al_2O_3–5 vol% SiC nano-composites. Therefore, the residual stress in the matrix generated by TEC mismatch between the matrix and inclusions has the largest value along the c-axis, and is lowest along the a-axis. Equation (5) can be used to substitute the TEC of the matrix in eqn (2) in the calculation of the constraint strain, when the residual stress in the composites can be related to specific orientations.

4 The Residual shear stress and dislocations

The mechanisms of stress relaxation are based on creep, dislocation generation and/or dislocation movement, which are all dependent on shear stress. The formation of dislocation bands by thermal annealing is a major contributor to the stress relaxation process. Hence, the maximum shear stress present in the matrix is an important parameter influencing stress relaxation, and can be calculated from:

$$\tau^M{}_{\max} = -\frac{3(r/R)^3}{4(1-F)}\,\sigma_I \qquad (6)$$

The direction for the maximum shear stress is at 45° from the radial direction. Figure 2 also shows the residual shear stress distribution in the matrix, and demonstrates that the residual shear stress near the particles is very high.

Figure 3 shows the TEM microstructure of an Al_2O_3–5 vol% SiC composite. The high strain contours (dark bands) are found surrounding the SiC particles, which indicates strong support for the assumptions made for the calculation. The level of residual shear stress is thus a function of both temperature and position. At room temperature, the maximum residual stress is approximately

Fig. 3. The microstructure of Al_2O_3–5 vol% SiC nano-composites, observed using TEM.

1500 MPa, which is much lower than the yield stress (at room temperature) of Al_2O_3. This residual stress is steadily built up during cooling down from the fabrication temperature. The yield stress of the alumina is considerably reduced at high temperature and would be expected to increase exponentially as the temperature decreases. Therefore, over a certain temperature range, the residual stress may well be higher than the yield stress, in which case dislocations will be generated and move at some point during the cooling cycle. Figure 4 compares the residual shear stress and the yield stresses of Al_2O_3. It should be noted that the stress plotted in Fig. 4 is not the residual shear stress but is the calculated shear stress increased by a factor of two in order to compare with the yield stress (or the resolved stress for basal and prism sliding). As can be seen from the figure, the maximum residual shear stress (at the particle–matrix interface) is greater than either of the

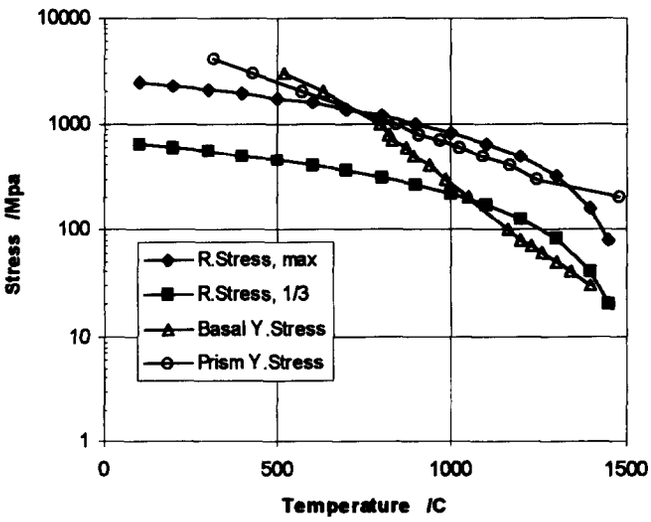

Fig. 4. Comparison of the residual shear stresses in the matrix and the resolved basal prismatic sliding stresses of Al_2O_3 over the temperature range 100–1450°C. The resolved stresses were obtained from Ref. 36.

resolved stresses required for dislocation movement at temperatures higher than 700°C. This indicates that both basal and prismatic slip can take place in Al_2O_3 grains in the nano-composites, initiated at the SiC interfaces. The residual shear stress at one-third of the shell thickness from the interface is also shown in Fig. 4, the stress being higher than the resolved stress for basal glide at temperatures higher than 1100°C. Hence, it is expected that both basal and prismatic dislocations would be generated in the matrix of Al_2O_3–5 vol% SiC nano-composites during cooling down from the fabrication temperature, and that the basal plane dislocations would be more readily generated, as observed by Jiao *et al.*[10]

Holding in the critical temperature range (such as 1300°C) will allow time for relaxation processes to occur and help develop the dislocation bands along specific directions, defined by high shear stress and low yield stress, to form 'sub-grain boundaries', as reported by Niihara *et al.*[1–3] Surface grinding of the nano-composites can introduce surface residual stress, as reported by the Lehigh University researchers and will further increase the chance of dislocation band formation in the composites, especially during subsequent thermal treatment.[12,13]

Formation of dislocations or the occurrence of creep deformation as a consequence of the high value of the maximum shear stress depends on the location of the inclusions in the composites. When the inclusions are present at the grain boundaries, the stress can be relieved by elastic accommodation, grain boundary sliding and diffusion-controlled processes. In the case where the inclusions are located in the grains, the diffusion rate is reduced and diffusion-controlled processes become more difficult, when shear-controlled mechanisms such as dislocation generation and movement, and twinning controlled stress relief mechanisms would be the preferred methods to accommodate the strain.

5 TEM observation

In order to confirm the analysis made above, that the dislocations in the matrix are generated by the large residual shear stress around the SiC particles, transmission electron microscopy has been used to examine the thermally annealed (at 1300°C) samples of the Al_2O_3–5 vol% SiC composite. Figure 5 shows a TEM micrograph of the sample. The dislocations necessary to relieve the residual stresses can be clearly observed in the Al_2O_3 grains. As predicted, the dislocations are initiated from the SiC particles. Certain of the dislocations are not fully developed, but others are well developed and can be seen to have undergone recovery processes to form the dislocation networks.

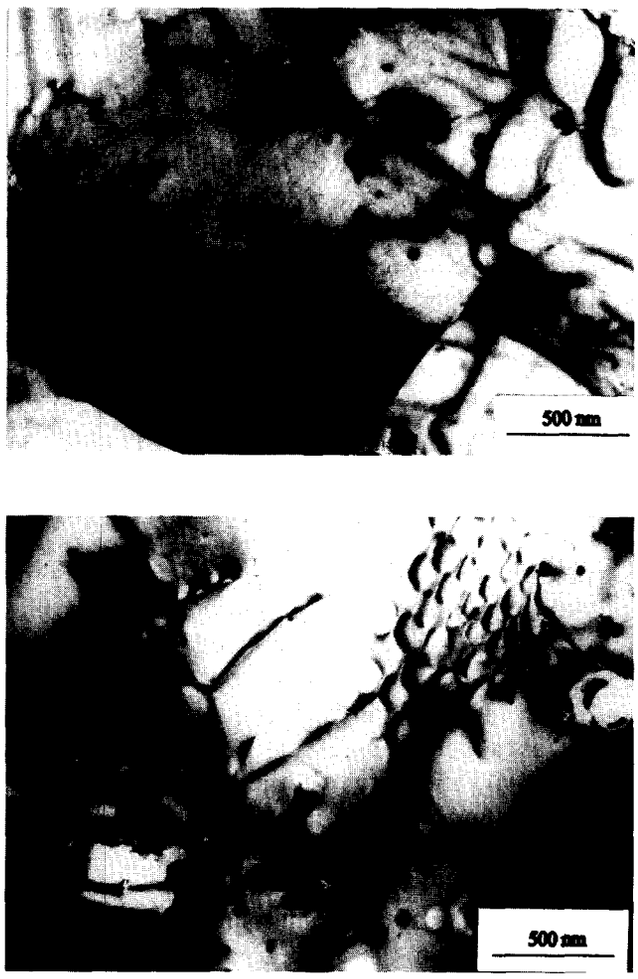

Fig. 5. Dislocations in the Al_2O_3 grains of thermally annealed Al_2O_3–5 vol% SiC nano-composites, annealing condition: 1300°C for 2 h.

There appear to be two types of network, the first the more common hexagonal dislocation network forming a sub-boundary as often found in annealed structures of many engineering materials and the second a tangle of dislocations initiated from and joining onto adjacent SiC particles.

6 Discussion

The strengthening in Al_2O_3–5 vol% SiC composites has been attributed by Zhao *et al.*[4] to a combination of the residual stress due to machining and crack healing. A residual machining stress is induced by the deformation generated by the surface grinding. At elevated temperature, grain boundary diffusion and sliding can take place to allow permanent deformation in ceramics. Thus in monolithic Al_2O_3, deformation taking place on annealing would be due to the residual machining stress generated near the surface and would manifest itself by grain boundary sliding.

High residual stresses, especially high residual shear stresses are present in the Al_2O_3 grains of the Al_2O_3–5 vol% SiC nano-composites, and dislocations are more likely to form and move in this environment than in the monolithic Al_2O_3. Thus two competitive processes take place in the composites due to the residual machining stress. The first is the permanent deformation generated by grain boundary sliding, the second the deformation generated by dislocations and dislocation movement in the matrix grains. It is much more difficult for grain boundary sliding to occur in the composite than in monolithic alumina, since the SiC nano-particles can sit on the grain boundaries, inhibiting the sliding. The high temperature creep experiment can confirm the pinning effect of the particles at the boundaries, inhibiting the sliding mechanisms; hence the creep rate of the composites is considerably lower than that of the monolithic material.[7,8] The second concerns the formation and movement of the dislocations in the matrix grains as a consequence of the residual stresses generated by mismatch of the thermal expansion coefficients and the machining stresses. In the composites this second mechanism predominates; the residual machining stress is present in the matrix grain rather than in the grain boundaries. The slower diffusion rates in the bulk result in the residual stresses becoming more difficult to relieve by thermal annealing than those present in the grain boundary as is the case in the monolithic alumina. Indentation residual stress relaxation both in the matrix and composite[12,13] would support this reasoning.

Whereas the indentation residual stresses in monolithic Al_2O_3 are completely relieved by thermal treatment at 1300°C, heating to the same temperature can only partially relieve the residual stresses in the nano-composites.[12,13] The indentation residual stress relaxation measurements have been extended further in the present set of experiments, when results have shown that the residual stresses in the nano-composites can be completely relieved by a thermal treatment at 1400°C for 2 h. Since the recovery/relaxation process in the composites occurs by dislocation movement in the matrix grains, the dislocations would tend to move to the grain boundaries or any crack tips or stress concentrations which lie within the grains. Since the thermal mismatch residual stresses decay rapidly away from the inclusions, it becomes difficult for the dislocations to move to the grain boundary over somewhat longer distances. The dislocations would tend to move over shorter distances to the crack tips, which can result in crack healing.[12,13] In this manner the thermal mismatch residual stresses play an important part in the crack healing.

Residual stresses generated by thermal mismatch may also induce microcracking on the surface of the composite during machining, but the microcracks would not be expected to propagate extensively, since the residual stresses are localised around the inclusions and also tend to be preferentially oriented (see Figure 2).

The fracture mode is also of relevance. The dislocation bands in the matrix grains are connected to SiC nano-particles and the high tensile loop residual stress generated by the thermal mismatch is also present around them. The manner in which cracks propagate would be dependent on the magnitude of the localised tensile stress. The high value of the residual tensile stress adjacent to the SiC nano-particles results in the dominant transgranular fracture mode in the nano-composites by connection of the propagating crack linking from one inclusion to another within the grains, as shown in Fig. 6.

In general, the transgranular fracture mode implies a low fracture toughness due to lack of crack deflection toughening, but in this case, the transgranular cracking is deflected by the stress field around the inclusions, as shown in Fig. 6, which illustrates the two-dimensional image. In the real three-dimensional case, cracks may also be pinned by the high radial compressive residual stress generated by inclusions which are close together. The compressive residual stress has two functions: increasing the possibility of cracking as shown in Fig. 6, and crack pinning. In addition, the presence of a compressive radial residual stress around the inclusions will decrease the possibility of interfacial debonding or cracking between the inclusion and the matrix. A further pinning effect is due to the SiC particles residing at and pinning

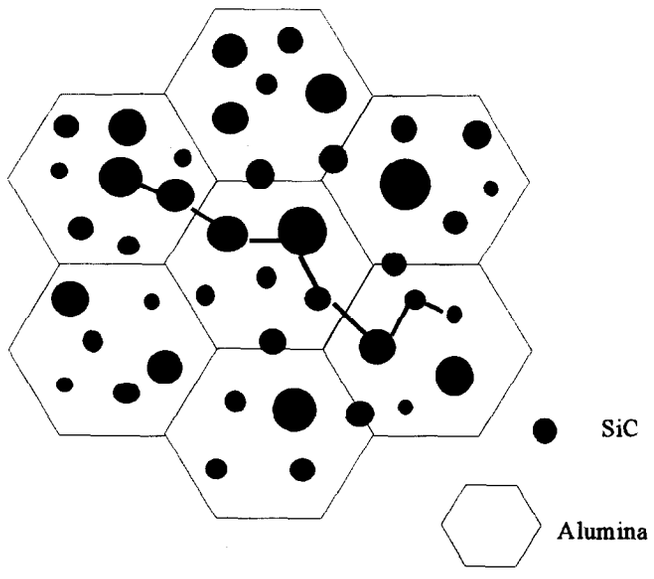

Fig. 6. A diagrammatic representation of the microstructure and the possible crack propagation in Al_2O_3–5 vol% SiC nano-composites.

the crack front, effectively causing crack bridging. The compressive radial residual stress explains the strength enhancement measured in the composites where the thermal expansion coefficient of the matrix is higher than that of the inclusions and where the overall residual stress in the matrix is tensile.

It is apparent that the toughening mechanisms in the nano-composites include crack bridging, crack deflection and crack pinning. The toughening increment due to crack bridging in the composites may not be high,[9] but the presence of a compressive residual stress can further increase the toughening effect. Taking into account the residual stress, a recalculation of the toughness increment by crack bridging in Al_2O_3–5 vol% SiC nano-composite, using eqn (14) in Ref. 9 gives:

$$K_{IC}{}^{C}/K_{IC}{}^{M} = 1 + 0{\cdot}07\phi,$$
ignoring the effect of the residual stress (7a)

$$K_{IC}{}^{C}/K_{IC}{}^{M} = 1 + 0{\cdot}25\phi,$$
considering the effect of the residual stress (7b)

where $K_{IC}{}^{C}$ and $K_{IC}{}^{M}$ are the fracture toughness of the composites and matrix, respectively. ϕ is a parameter related to the bridging length, increasing with bridging length. The presence of a compressive radial stress will further increase the bridging length, which generates higher values of ϕ and hence toughness, in eqn (7b).

In summary, the phenomena observed in Al_2O_3–5 vol% SiC nano-composites are quite different from those which occur in monolithic Al_2O_3. The dominant factor responsible for the difference is the occurrence of residual stresses in the composites generated by the mismatch of the thermal expansion coefficients between Al_2O_3 and SiC. The presence of residual stress manifests itself in the generation and movement of dislocations, a change in fracture mode, and an increase in strength and toughness. More detailed work is required to evaluate quantitatively the strength and toughness increments in the composite.

References

1. Niihara, K. and Nakahira, A., In *Advanced Structural Inorganic Composites*, ed. P. Vincenzini. Elsevier Science Publishers, London, 1991, pp. 637–644.
2. Niihara, K., *J. Ceram. Soc. Japan*, 1991, **99**, 974.
3. Nakahira, A. and Niihara, K., In *Fracture Mechanics of Ceramics*, Vol. 9, ed. R. C. Bradt *et al.* Plenum Press, New York, 1992, pp. 165–177.
4. Zhao, J., Sterns, L. C., Harmer, M. P., Chan, H. M. and Miller, G. A., *J. Am. Ceram. Soc.*, 1993, **76**, 503.
5. Borsa, C. E., Jiao, S., Todd, R. I. and Brook, R. J., *J. Microscopy*, 1995, **177**, 305.
6. Wohlfromm, H., In *Ceramic Transactions*, Vol. 51: *Ceramic Processing Science and Technology*. American Ceramic Society, 1995, pp. 659–663.
7. Ohji, T., Nakahira, A., Hirano, T. and Niihara, K., *J. Am. Ceram. Soc.*, 1994, 77, 3259.
8. Thompson, A. M., Fang, J., Chan, H. M. and Harmer, M. P., In *Ceramic Transactions*, Vol. 51: *Ceramic Processing Science and Technology*. American Ceramic Society, 1995, pp. 671–679.
9. Pezzotti, G., Nishida, T. and Sakai, M., *J. Ceram. Soc. Japan*, 1995, **103**, 901.
10. Jiao, S., Borsa, C. E. and Walker, C. N., *Silicates Industries*, 1995, **7–8**, 211.
11. Levin, I., Kaplan, W. D., Brandon, D. G. and Wieder, T., *Acta Metal. Mater.*, 1994, **42**, 1147.
12. Fang, J., Chan, H. M. and Harmer, M. P., *Mater. Sci. Eng.*, 1995, **A195**, 163.
13. Thompson, A. M., Chan, H. M., Harmer, M. P. and Cook, R. F., *J. Am. Ceram. Soc.*, 1995, **78**, 567.
14. Chou, I. A., Chan, H. M. and Harmer, M. P., *J. Am. Ceram. Soc.*, 1996, **79**, 2403.
15. Todd, R. I., Bourke, M. A. M., Borsa, C. E. and Brook, R. J., In *Fourth EuroCeramics*, Vol. 4, ed. A. Bellosi. Gruppo Editoriale Faenza, Faenza, 1995, pp. 217–224.
16. Pezzotti, G., Sergo, V., Ota, K., Sbaizero, O., Muraki, N., Nishida, T. and Sakai, M., *J. Ceram. Soc. Japan*, 1996, **104**, 497.
17. Eshelby, J. D., *Proc. Roy. Soc. London*, 1957, **A241**, 376.
18. Mori, T. and Tanaka, K., *Acta Metall.*, 1973, **21**, 571.
19. Mura, T. (ed), *Micromechanics of Defects in Solids*, Hijhoff, The Hague, 1982.
20. Luo, J. and Stevens, R., *J. Appl. Phys.*, 1996, **79**, 9047.
21. Lambrecht, W. R. L., Segall, B., Methfessel, M. and Vanschilfgaarde, M., *Phys. Review B—Condens. Matter.*, 1991, **44**, 3685.
22. Tang, M. J. and Yip, S., *Phys. Review B—Condens. Matter.*, 1995, **52**, 15150.
23. Fukuhara, M. and Yamauchi, I., *J. Mater. Sci.*, 1993, **28**, 4681.
24. Repelin, Y., Husson, E. and Proust, C., *J. Solid State Chem.*, 1995, **116**, 378.
25. Simmons, G. and Wang, H. (eds), *Single crystal elastic constants and calculated aggregate properties*. MIT Press, Cambridge, MA, 1971.
26. Li, Z. and Bradt, R., *J. Am. Ceram. Soc.*, 1986, **69**, 863.
27. Li, Z. and Bradt, R., *J. Appl. Phys.*, 1986, **60**, 612.
28. Li, Z. and Bradt, R., *J. Mater. Sci.*, 1986, **21**, 4366.
29. Li, Z. and Bradt, R., In *Ceramic Transactions*, Vol. 2: *Silicon Carbide '87*, ed. J. D. Cawleyand and C. E. Semler. 1989, pp. 313–339.
30. Wachtman, J. B. Jr., Scuderl, T. G. and Cleek, G. W., *J. Am. Ceram. Soc.*, 1962, **45**, 319.
31. Dorr, E. and Hubner, H., ed., Alumina: Processing, Properties and Applications. Springer-Verlag, Berlin, 1984.
32. Morrell, R., (ed.), *Handbook of properties of technical and engineering ceramics*, Part 1: *An introduction for the engineer and designer*. Her Majesty's Stationery Office, London, 1985.
33. Morrell, R. (ed.), *Handbook of properties of technical and engineering ceramics*, Part 2: *Data reviews, Section I, High-alumina ceramics*. Her Majesty's Stationery Office, London, 1987.
34. Evans, A. G. and Fu, F., In *Fracture in Ceramic Materials: Toughening Mechanisms, Machining Damage, Shock*, ed. A. G. Evans. Noyes Publications, New Jersey, 1984.
35. Hashin, Z., *J. Appl. Mech.*, 1962, **29**, 143.
36. Wang, T. T. and Kwei, T. K., *J. Polymer Sci.*, 1969, **A7**, 889.
37. Cannon, R. M., In *Advances in Ceramics*, Vol. 10, *Structure and Properties of MgO and Al_2O_3 Ceramics*, ed. W. D. Kingery. American Ceramic Society, 1984.

Appendix: Composite Sphere Model (CSM)

The CSM model is based on the assumption that the inclusion composite can be represented by a collection of many tiny spherical composites of

various sizes. Each of the spherical composites contains a inclusion and a concentric spherical shell of matrix. The volume fraction of the inclusion in each spherical composite is the same as the total volume fraction of the inclusions in the matrix. Hence, the thickness of the shell is given by:

$$t = rF^{-1/3}(1 - F^{1/3})$$

(r is the radius of the spherical inclusion).

Hashin[35] first used the composite sphere model to evaluate the elastic moduli of heterogeneous materials. Wang and Kwei,[34] developed the application to analyse the overall thermal expansion coefficient of composite materials. The displacement mismatch on the interface between the matrix and the inclusions is given by:

$$\Delta u = r\varepsilon^T.$$

The boundary conditions are:

$$u^I(0) = 0, \qquad u^I(r) = u^M(r),$$
$$\sigma_r^I(r) = \sigma_r^M(r), \qquad \sigma_r^M(r+t) = 0$$

The residual stresses in the inclusions generated by the mismatch can be calculated, using the same relationship expressed in eqn (1b), indirectly confirming that the CSM model is an acceptable method for the evaluation of the residual stress. The residual stresses in the matrix are expressed by eqn (4).